

# Microscopic study of Gamow-Teller and spin-dipole states in $^{208}\text{Bi}$

T. Suzuki<sup>1,a</sup> and H. Sagawa<sup>2,b</sup><sup>1</sup> Department of Physics, College of Humanities and Sciences, Nihon University Sakurajosui 3-25-40, Setagaya-ku, Tokyo 156, Japan<sup>2</sup> Center for Mathematical Sciences, the University of Aizu Aizu-Wakamatsu, Fukushima 965, Japan

Received: 11 April 2000 / Revised version: 1 August 2000

Communicated by: P. Schuck

**Abstract.** Gamow-Teller (GT) and spin-dipole (SD) states in  $^{208}\text{Bi}$  are studied by using self-consistent Hartree-Fock + Tamm-Dancoff approximation taking into account the coupling to the continuum. Most of SD strength is found at the excitation energy  $E_x \approx 25$  MeV with a very broad width, which agrees with recent experimental observations. It is shown that Landau damping effect is responsible for the large width of SD peak, while the escape width is found to be at most 1 MeV. We study also electric dipole ( $E1$ ) transitions between GT and SD states in  $^{208}\text{Bi}$ . Main  $E1$  transitions for  $0^-$  and  $1^-$  states are found near excitation energy expected from Brink's hypothesis in which SD states are considered as  $E1$  resonances built on the GT state. Calculated  $E1$  transition strengths between GT and SD states are compared with the analytic sum rules within one-particle one-hole (1p-1h) configuration space and within both 1p-1h and 2p-2h model space.

**PACS.** 24.30.Cz Giant resonances – 21.10.Pc Single-particle levels and strength functions – 23.20.Lv Gamma transitions and level energies – 21.60.Jz Hartree-Fock and random-phase approximations

## 1 Introduction

Spin excitation modes in nuclei such as magnetic dipole (M1), Gamow-Teller (GT) and spin-dipole (SD) excitations have been studied intensively both theoretically [1–5] and experimentally [6–10] in a broad region of mass chart. Especially the quenching and spreading of M1 and GT strength are interesting and stimulating subject under intensive study. Recently, the sum rule strength of GT transitions of  $^{90}\text{Nb}$  was studied quantitatively by charge exchange reactions [7], and the importance of the coupling to many-particle and many-hole states was pointed out on the quenching of the transition strength. Experimental investigations of GT and SD strengths in  $^{208}\text{Bi}$  have been done also at RCNP by  $^{208}\text{Pb}(^3\text{He},t)^{208}\text{Bi}$  reactions [8]. The width of SD peak is found to be about 8 MeV, which is twice as large as that of GT in  $^{208}\text{Bi}$ .

As a theoretical model, the self-consistent Hartree-Fock (HF) + random phase approximation (RPA) or Tamm-Dancoff approximation (TDA) has been extensively applied for giant resonances in a broad region of mass table [11,12]. The same model was used for the spin dependent excitations [2,3,13,14]. It was shown that the model predicts successfully GT and SD states in  $^{48}\text{Sc}$  and  $^{90}\text{Nb}$  [3,13]. The electric dipole ( $E1$ ) transitions between

GT and SD states in  $^{48}\text{Sc}$  and  $^{90}\text{Nb}$  were also studied in the same model [13]. In this paper, we study the GT and SD states by using the self-consistent HF + TDA model in  $^{208}\text{Bi}$ . Especially, we would like to clarify the physical mechanism of the observed large width of SD strength in comparison with theoretical results. In order to obtain the effect of the continuum width, we calculate also the coupling to the continuum of SD strength in the self-consistent TDA model in the coordinate space. In section 2, we formulate the sum rules of GT and SD strength, and that of  $E1$  transitions between them. The results of the self-consistent HF+TDA model are discussed in section 3. A summary is given in section 4.

## 2 Sum rules for GT and SD strength and $E1$ transitions between them

Sum rules are useful tools to study collective nature of excitation modes in many-body systems. Particularly, for the charge exchange excitations, model independent sum rules are derived and used to analyse experimental data. We summarize various sum rules for spin-dependent charge exchange excitations in the following. The operators for GT, SD and  $E1$  transitions are defined by

$$\hat{G}_{\pm} = \sum_{im} \tau_{\pm}^i \sigma_m^i,$$

<sup>a</sup> e-mail: [suzuki@chs.nihon-u.ac.jp](mailto:suzuki@chs.nihon-u.ac.jp)<sup>b</sup> e-mail: [sagawa@u-aizu.ac.jp](mailto:sagawa@u-aizu.ac.jp)

$$\begin{aligned}\hat{S}_{\pm} &= \sum_{im\mu} \tau_{\pm}^i \sigma_m^i r_i Y_1^{\mu}(\hat{r}_i), \\ \hat{D} &= \sum_{i\mu} \frac{1}{2} \tau_3 r_i Y_1^{\mu}(\hat{r}_i),\end{aligned}\quad (1)$$

respectively, with the isospin operators  $\tau_3 = \tau_z, \tau_{\pm} = \frac{1}{2}(\tau_x \pm i\tau_y)$ . The model independent sum rule for the GT transitions is expressed as

$$\begin{aligned}G_- - G_+ &= \sum_{i \in \text{all}} |\langle i | \hat{G}_- | 0 \rangle|^2 - \sum_{i \in \text{all}} |\langle i | \hat{G}_+ | 0 \rangle|^2 \\ &= \langle 0 | [\hat{G}_-, \hat{G}_+] | 0 \rangle = 3(N - Z)\end{aligned}\quad (2)$$

The model independent sum rule for the SD  $\lambda$ -pole operator  $\hat{S}_{\pm}^{\lambda} = \sum_i \tau_{\pm}^i r_i [\sigma \times Y_1(\hat{r}_i)]^{\lambda}$  also can be derived to be

$$\begin{aligned}S_-^{\lambda} - S_+^{\lambda} &= \sum_{i \in \text{all}} |\langle i | \hat{S}_-^{\lambda} | 0 \rangle|^2 - \sum_{i \in \text{all}} |\langle i | \hat{S}_+^{\lambda} | 0 \rangle|^2 \\ &= \langle 0 | [\hat{S}_-^{\lambda}, \hat{S}_+^{\lambda}] | 0 \rangle = \frac{(2\lambda + 1)}{4\pi} (N \langle r^2 \rangle_n - Z \langle r^2 \rangle_p).\end{aligned}\quad (3)$$

An analytic formula for the total  $E1$  transition rates between GT and SD states is derived in the TDA framework [13] by using the doorway states,

$$|GT\rangle = \frac{1}{\sqrt{N_{\text{GT}}}} \hat{G}_- | 0 \rangle, \quad (4)$$

$$|SD\rangle = \frac{1}{\sqrt{N_{\text{SD}}}} \hat{S}_- | 0 \rangle, \quad (5)$$

where  $|0\rangle$  is the parent state and  $N_{\text{GT}} = \langle 0 | \hat{G}_+ \hat{G}_- | 0 \rangle$  and  $N_{\text{SD}} = \langle 0 | \hat{S}_+ \hat{S}_- | 0 \rangle$  are the normalization factors. Then, the total  $E1$  transition rate can be evaluated within the 1p-1h configuration space as

$$\begin{aligned}S_{1\text{p-1h}} &= |\langle 0 | \hat{S}_+ \hat{D} \hat{G}_- | 0 \rangle|^2 / [\langle 0 | \hat{G}_+ \hat{G}_- | 0 \rangle \langle 0 | \hat{S}_+ \hat{S}_- | 0 \rangle] \\ &= [6 \langle 0 | \hat{D}^{\dagger} \hat{D} | 0 \rangle - \langle 0 | \hat{S}_+ \hat{S}_- | 0 \rangle]^2 \\ &\quad / [3(N - Z) \langle 0 | \hat{S}_+ \hat{S}_- | 0 \rangle].\end{aligned}\quad (6)$$

It is interesting to notice that the total  $E1$  transition rate between the GT and SD states in the daughter nucleus is related in eq. (6) to the rates of  $E1$  and SD transitions in the parent nucleus. The sum of all possible  $E1$  transitions from the GT state to 1p-1h and 2p-2h states was also derived to be [13]:

$$\begin{aligned}S_A &= \sum_{i \in \text{all}} |\langle i | \hat{D} \hat{G}_- | 0 \rangle|^2 \frac{1}{N_{\text{GT}}} \\ &= \langle 0 | \hat{G}_+ \hat{D}^{\dagger} \hat{D} \hat{G}_- | 0 \rangle / \langle 0 | \hat{G}_+ \hat{G}_- | 0 \rangle \\ &= \langle 0 | \hat{D}^{\dagger} \hat{D} | 0 \rangle\end{aligned}\quad (7)$$

One can see in eq. (7) that the sum of the  $E1$  transition strength from the GT state is equal to that from the ground state in the parent nucleus.

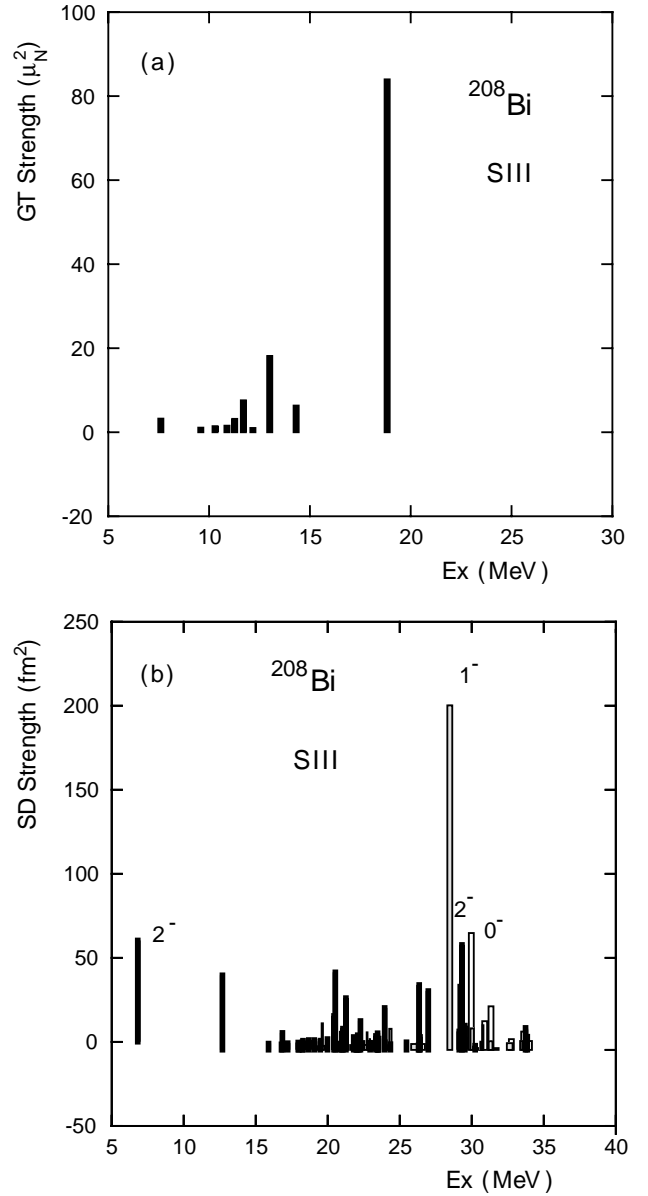


**Fig. 1.** GT and SD states calculated by discrete HF+TDA model with SIII interaction: (a) GT transition strength from the parent ground state  $^{208}\text{Pb}$  to GT states in  $^{208}\text{Bi}$ . (b) SD transition strength from the parent ground state  $^{208}\text{Pb}$  to SD states in  $^{208}\text{Bi}$ . The excitation energy is measured from the ground state of  $^{208}\text{Pb}$ .

### 3 Numerical results

Calculated results of GT and SD strengths in  $^{208}\text{Bi}$  obtained by HF + TDA with the use of discrete basis and the SIII interaction [15] are shown in fig. 1. We performed also RPA calculations of GT and SD transitions with discrete basis and found almost the same results as those of TDA. Because of the large excess neutrons in  $^{208}\text{Pb}$ , the backward amplitudes of RPA are blocked for almost all GT and SD configurations. Calculated GT state is located at energy of  $E_x = 18.8\text{ MeV}$  with respect to the parent, and 63.6 % of the total strength is

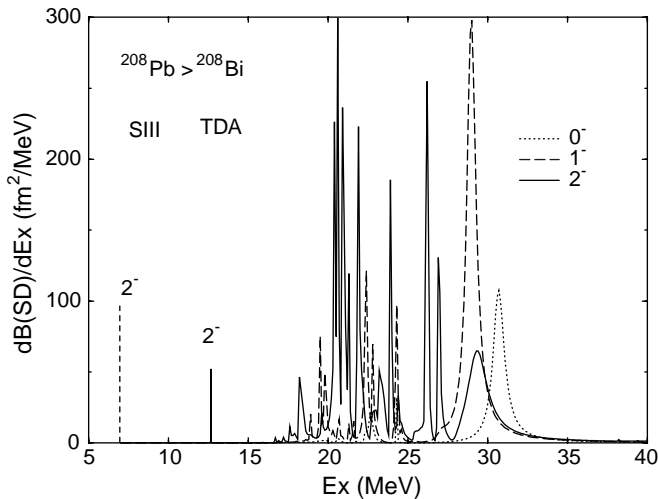


**Fig. 2.** SD transition strength in  $^{208}\text{Bi}$  calculated by continuum HF+TDA model with SIII interaction. The dotted, dashed and solid curves show the response of  $0^-$ ,  $1^-$  and  $2^-$ , respectively. The  $2^-$  state at  $E_x = 6.81$  MeV is below the proton threshold and shown by a dashed line. The excitation energy is measured from the ground state of  $^{208}\text{Pb}$ .

concentrated in the state. The energy obtained for the GT state shows good agreement with the experimental one,  $E_x = 19.2 \pm 0.2$  MeV [8]. The SD strengths for  $0^-$  and  $1^-$  states are concentrated in one state with more than 40% probabilities, while that for  $2^-$  states are fragmented among many states. There are low-lying  $2^-$  states at  $E_x = 6.8$  MeV and 12.7 MeV. These states are mainly formed of  $\pi 0h_{9/2}\nu 0i_{13/2}^{-1}$  and  $\pi 0i_{13/2}\nu 0h_{9/2}^{-1}$  configurations, respectively. The former state can have a large E1 transition matrix element with the GT state while the latter one cannot (see fig. 4 also). Sum of the calculated SD strengths are  $160 \text{ fm}^2$ ,  $427 \text{ fm}^2$  and  $649 \text{ fm}^2$  for  $J = 0^-$ ,  $1^-$  and  $2^-$  states, respectively. The ratio is roughly proportional to  $2J+1$ . The total sum of the strength gives  $\langle 0|\hat{S}^\dagger\hat{S}|0\rangle = 1236.4 \text{ fm}^2$ . Similar strength distributions with the energy shift of about 2 MeV upward are obtained with the use of the SGII interaction [2] for both the GT and SD states. The model independent sum rule for the SD transitions (3) can be given for  $^{208}\text{Pb}$  as

$$S_-^\lambda - S_+^\lambda = \begin{cases} 121 \text{ fm}^2 & \lambda = 0^- \\ 363 \text{ fm}^2 & \lambda = 1^- \\ 604 \text{ fm}^2 & \lambda = 2^- \end{cases}, \quad (8)$$

using HF radii with SIII interaction. The  $S_+^\lambda$  contributions to the sum rule (8) are found to be  $39 \text{ fm}^2$  for  $0^-$ ,  $64 \text{ fm}^2$  for  $1^-$  and  $45 \text{ fm}^2$  for  $2^-$ , respectively.

We have done also continuum HF+TDA calculations in the coordinate space with the same SIII interaction. Detailed descriptions of the model can be found elsewhere [12]. Calculated results for SD strength are shown in fig. 2. Characteristic features of the distribution and magnitude of the strength are not altered from those obtained by the discrete TDA calculations. The escape width  $\Gamma^\uparrow$  is negligible below  $E_x \approx 15$  MeV, while it becomes about a

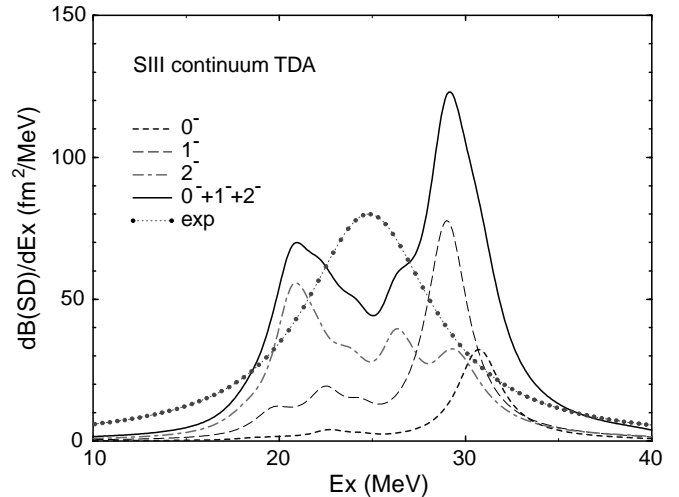


**Fig. 3.** Averaged SD transition strength (9) in  $^{208}\text{Bi}$  calculated with a weighting factor (10) for continuum HF+TDA results in fig. 2. Experimental data are taken from [8]. The absolute magnitude of the experimental data is in an arbitrary unit. The excitation energy is measured from the ground state of  $^{208}\text{Pb}$ .

few hundreds keV in the energy region  $E_x = (17-27)$  MeV. We can see large peaks at around  $E_x = 30$  MeV for all  $J = 0^-$ ,  $1^-$  and  $2^-$  responses. Integrated transition strength of each peak is  $135 \text{ fm}^2$  for  $0^-$ ,  $309 \text{ fm}^2$  for  $1^-$  and  $130 \text{ fm}^2$  for  $2^-$  which exhausts 84%, 72 % and 20% of the corresponding total strength, respectively. We should notice in fig. 2 that the high energy peaks obtain more strength than the discrete TDA calculations due to the coupling to the continuum. The widths of these peaks are about 1 MeV, which are substantially larger than those of lower energy peaks. Most of the SD strength distributes in a wide energy region between  $E_x = 20$  and 33 MeV, except for the two low-lying  $2^-$  states at  $E_x = 6.8$  and 12.7 MeV.

In fig. 3, the experimental data is shown together with averaged results of continuum TDA calculations. The averaged results are obtained by using a weighting factor  $\rho$ ,

$$\frac{dB(SD)_{\text{ave}}}{dE_x} = \int \frac{dB(SD)}{dE'_x} \rho(E'_x - E_x) dE'_x \quad (9)$$

where

$$\rho(E'_x - E_x) = \frac{1}{\pi} \frac{\Delta/2}{(E'_x - E_x)^2 + (\Delta/2)^2} \quad (10)$$

with  $\Delta=2$  MeV. The calculated strength shows structure of two peaks, in which the lower (higher) one is dominated by  $2^-$  ( $1^-$ ) states. The height of  $0^-$  peak is about a factor two smaller than that of  $1^-$  centered at  $E_x \sim 30$  MeV. The low-lying  $2^-$  state at  $E_x = 12.7$  MeV with single particle-hole nature is smeared out by the averaging. Experimentally, a broad SD bump in  $^{208}\text{Bi}$  is found recently by  $^{208}\text{Pb}(^3\text{He}, t)^{208}\text{Bi}$  reaction centered at  $E_x = 24.8 \pm 0.8$  MeV with a very large total width of  $8.4 \pm 1.7$  MeV [8]. Because of relatively poor statistics of the  $^{208}\text{Pb}(^3\text{He}, t)^{208}\text{Bi}$  reactions, it is rather difficult to

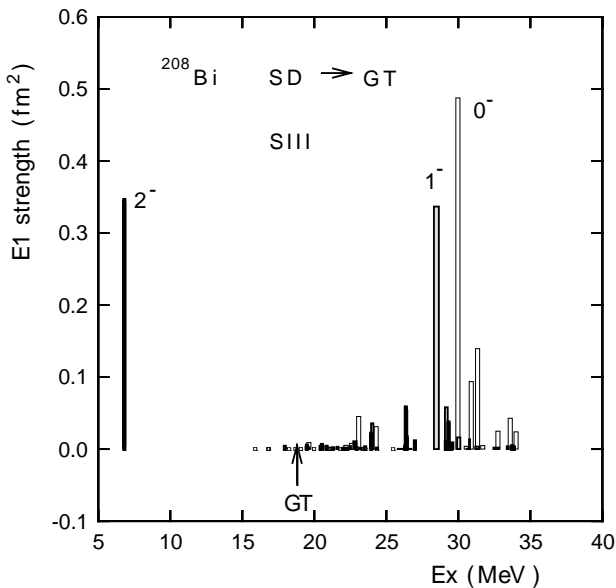


**Fig. 4.** Electric dipole transition strength from the SD states to the main GT state in  $^{208}\text{Bi}$ .

see detailed structure of SD strength in the experimental spectra. On the average, however, the calculated results show good agreement with the experimental observations as far as the excitation energy and the width are concerned though the two peak structure obtained by the calculation is not seen in the observation. Notice that main part of the calculated width is due to the Landau damping effect together with the coupling to the continuum. The latter effect is at most 1 MeV in the higher energy region than  $E_x = 27$  MeV and plays a minor role on the width of SD resonance. The effect of the coupling to the many-particle many-hole states on the width might be simulated by the weighting factor (10) with the width of  $\Delta=2$  MeV. A quantitative agreement between the calculated and the empirical width suggests that the width  $\Gamma^\downarrow$  due to the coupling to many-particle many-hole states will be a magnitude of 2 MeV in the case of SD resonances in  $^{208}\text{Bi}$ . The absolute strength of the experimental data is shown in an arbitrary unit in fig. 3 since the sum rule value is not yet reported.

In  $^{90}\text{Zr}$ , the SD strengths have been studied with RPA model including 2p-2h states [16]. It was found that mixing between 1p-1h and 2p-2h states results in a large asymmetric spreading of the strength of the SD resonances, with about 30% of the total strength shifted to excitation energies greater than 35 MeV.

Calculated  $E1$  transition strengths from the SD states to the GT state at  $E_x = 18.83$  MeV obtained with the use of the SIII interaction are shown in fig. 4. Here, the effective charge is taken to be  $N/A$  e for protons and  $-Z/A$  e for neutrons. The SD strength for  $1^-$  is concentrated almost in one state at  $E_x = 28.5$  MeV with 63% probability. For  $0^-$ , most of the strength is found among a few states at  $E_x \sim 30$  MeV. For  $2^-$ , half of the strength is fragmented among many states at  $E_x = 15 \sim 30$  MeV while a state at  $E_x = 6.8$  MeV exhausts 53% of the strength.

Sum of the  $E1$  strength for each multipole is calculated to be  $0.920$  fm $^2$ ,  $0.531$  fm $^2$  and  $0.548$  fm $^2$  for  $0^-$ ,  $1^-$  and  $2^-$ , respectively. The value  $S_{1p-1h}$  in eq. (6) is equal to  $2.40$  fm $^2$  as one obtains  $\langle 0 | \hat{D}^\dagger \hat{D} | 0 \rangle = 101.7$  fm $^2$  for the total  $E1$  transition rate in  $^{208}\text{Pb}$  and  $\langle 0 | \hat{S}_+ \hat{S}_- | 0 \rangle = 1236.4$  fm $^2$  for the sum of the SD strengths in  $^{208}\text{Pb}$ . The total  $E1$  transition strength from the collective GT state at  $E_x = 18.8$  MeV to all the SD states is  $1.750$  fm $^2$ , which amounts to be 72.9 % of the sum rule  $S_{1p-1h}$  in eq. (6). The transition rate from the GT state at  $E_x = 18.8$  MeV to the each SD multipole is 17.5 %, 30.3 % and 52.2 % of the total rate ( $= 1.750$  fm $^2$ ) for  $0^-$ ,  $1^-$  and  $2^-$ , respectively. Strong  $E1$  transition rates are calculated to be  $0.34 \sim 0.49$  e $^2$ fm $^2$ , which are 15  $\sim$  22% of the Weisskopf unit ( $2.26$  e $^2$ fm $^2$ ) for  $^{208}\text{Bi}$ . This order of magnitude of the transition strength might be easily accessed experimentally. We should notice that the sum rule  $S_A$  of (7) for the 1p-1h and 2p-2h model space is  $101.7$ fm $^2$ , which is much larger than that within the 1p-1h model space. Thus the predicted  $E1$  strength in fig. 4 might be altered significantly by the effect of 2p-2h states. The measurement of  $E1$  strength from SD states might show clear empirical information of the 2p-2h states in  $^{208}\text{Bi}$ , which couple to both SD and GT states.

Finally, we comment on Brink's hypothesis [17] in which giant resonances can be built on top of any excited state besides the ground state. SD states can be considered as giant dipole states (GDR) on top of the excited GT states. The experimental systematic energy of GDR is given by  $E_x = 78/A^{1/3}$  MeV, which is 13.2 MeV for  $^{208}\text{Bi}$ . The major  $E1$  strength is found at around  $E_x = 30$  MeV in fig. 4, which is about 12 MeV above the GT state and close to the experimental energy of GDR measured from the GT states. Although Brink's hypothesis [17] seems to be valid in the present case, we should make a study including 2p-2h configurations to draw a definite conclusion.

## 4 Summary

We have investigated the GT and SD states in  $^{208}\text{Bi}$  using the self-consistent HF + TDA model within the 1p-1h configuration space both with the discrete basis and with the coupling to the continuum. The calculated excitation energy of main GT state is at 18.8 MeV which agrees with the experimental peak at  $19.2 \pm 0.2$  MeV. We showed also that the calculated SD strength gives good agreement with the observed data by  $^{208}\text{Pb}(^3\text{He}, t)^{208}\text{Bi}$  as far as the excitation energy and the width are concerned. The Landau damping effect is shown to be highly responsible for the large observed width of SD resonance, while the couplings to the continuum and to the many-particle and many-hole states play minor roles. The  $E1$  transition strength between the GT and SD states is evaluated in the same TDA model. The total  $E1$  strength from the GT to all the SD states is found to be  $1.75$  fm $^2$  within the 1p-1h model, which is about 1 Weisskopf unit of  $E1$  transition. Possible observed  $E1$  strength might be significantly enhanced due to the effect of 2p-2h states as is expected from

much larger value of the total  $E1$  sum rule  $S_A$  compared to that of  $S_{1p-1h}$  in  $1p-1h$  model space. The experimental observation of the  $E1$  transitions will be useful to obtain information on  $2p-2h$  configurations which couple to SD and GT states.

The authors would like express their thanks to M. Fujiwara and A. Krasznahorkau for informing them of the present experimental situation on the subject. This work was supported in part by Grant-in-Aid for Scientific Research (C) (Nos. 08640390 and 09640369) from the Ministry of Education, Science and Culture.

## References

1. G.F. Bertsch and I. Hamamoto, Phys. Rev. C **26**, 1323 (1982).  
K. Takayanagi, K. Shimizu and A. Arima, Nucl. Phys. A **447**, 205 (1988); A **481**, 313 (1988).  
S. Drożdż, S. Nishizaki, J. Speth and J. Wambach, Phys. Rep. **197**, 1 (1990).  
N.D. Dang, A. Arima, T. Suzuki and S. Yamaji, Nucl. Phys. A **621**, 719 (1997); Phys. Rev. Lett. **79**, 1638 (1997).
2. Nguyen Van Giai and H. Sagawa, Phys. Lett. B **106**, 379 (1981).
3. G. Colò, Nguyen Van Giai, P.F. Bortignon and R.A. Broglia, Phys. Rev. C **50**, 1496 (1992).
4. T. Suzuki and H. Sagawa, Nucl. Phys. A **637**, 547 (1998).
5. F. Osterfeld, Rev. Mod. Phys. **64**, 491 (1992);  
N. Auerbach and A. Klein, Phys. Rev. C **30**, 1032 (1984);  
F. Osterfeld, S. Krewald, H. Dermawan and J. Speth, Phys. Lett. B **105**, 257 (1981).
6. C. Gaarde, Nucl. Phys. A **369**, 127c (1983) and references therein.
7. T. Wakasa et al., Phys. Rev. C **55**, 2909 (1997);  
H. Sakai, H. Okamura, H. Otsu, T. Wakasa, S. Ishida, N. Sakamoto, T. Uesaka, Y. Satou, S. Fujita and K. Hatanaka, Nucl. Instrum. Methods Phys. Res. A **369**, 120 (1996).
8. H. Akimune et al., Phys. Rev. C **52**, 604 (1995);  
H. Akimune, I. Daito, Y. Fujita, M. Fujiwara, M.N. Harakeh, J. Janecke and M. Yosoi, Phys. Rev. C **61**, 011304(R) (2000) 011304(R).
9. M. Fujiwara et al., Nucl. Phys. A **599**, 223 (1996);  
Y. Fujita et al., Phys. Lett. B **365**, 29 (1996);  
H. Akimune, H. Ejiri, M. Fujiwara, I. Daito, T. Inomata, R. Hazama, A. Tamii, H. Toyokawa and M. Yosoi, Phys. Lett. B **394**, 23 (1997).
10. H. Okamura et al., Nucl. Phys. A **577**, 89 (1994);  
T. Ichihara et al., Nucl. Phys. A **577**, 93 (1994);  
M. Moinester et al., Phys. Lett. B **230**, 41 (1989).
11. G.F. Bertsch and S.F. Tsai, Phys. Rep. **18**, 125 (1975);  
K.F. Liu and G.E. Brown, Nucl. Phys. A **265**, 385 (1976);  
K.F. Liu and Nguyen Van Giai, Phys. Lett. B **65**, 23 (1976).
12. I. Hamamoto, H. Sagawa and X.Z. Zhang, Phys. Rev. C **55**, 2361 (1997).
13. T. Suzuki, H. Sagawa and Nguyen Van Giai, Phys. Rev. C **57**, 139 (1998).
14. I. Hamamoto and H. Sagawa, Phys. Rev. C **60**, 064314 (2000).
15. M. Beiner, H. Flocard, Nguyen Van Giai and P. Quentin, Nucl. Phys. A **238**, 29 (1975).
16. S. Drożdż, F. Osterfeld, J. Speth and J. Wambach, Phys. Lett. B **189**, 271 (1987).
17. D.M. Brink, PhD thesis (University of Oxford, 1955).